Published online 25 October 2007 *Nucleic Acids Research, 2007, Vol. 35, No. 21* ***7389–7395***
doi:10.1093/nar/gkm898

Domain I of ribosomal protein L1 is sufficient for specific RNA binding

Svetlana Tishchenko[1], Ekaterina Nikonova[1], Vladislav Kljashtorny[1], Olga Kostareva[1], Natalia Nevskaya[1], Wolfgang Piendl[2,*], Natalia Davydova[3], Victor Streltsov[4], Maria Garber[1] and Stanislav Nikonov[1]

[1]Institute of Protein Research, Russian Academy of Sciences, 142290 Pushchino, Moscow region, Russia, [2]Biocenter, Division of Medical Biochemistry, Innsbruck Medical University, Fritz-Pregl-Str. 3, 6020 Innsbruck, Austria, [3]Angiogenesis Laboratory, Ludwig Institute for Cancer Research, PO Box 2008, Royal Melbourne Hospital, Parkville, VIC 3050 and [4]CSIRO Molecular & Health Technologies 343 Royal Parade Parkville VIC 3052, Australia

Received August 9, 2007; Revised and Accepted October 4, 2007

ABSTRACT

Ribosomal protein L1 has a dual function as a ribosomal protein binding 23S rRNA and as a translational repressor binding its mRNA. L1 is a two-domain protein with N- and C-termini located in domain I. Earlier it was shown that L1 interacts with the same targets on both rRNA and mRNA mainly through domain I. We have suggested that domain I is necessary and sufficient for specific RNA-binding by L1. To test this hypothesis, a truncation mutant of L1 from *Thermus thermophilus*, representing domain I, was constructed by deletion of the central part of the L1 sequence, which corresponds to domain II. It was shown that the isolated domain I forms stable complexes with specific fragments of both rRNA and mRNA. The crystal structure of the isolated domain I was determined and compared with the structure of this domain within the intact protein L1. This comparison revealed a close similarity of both structures. Our results confirm our suggestion that in protein L1 its domain I alone is sufficient for specific RNA binding, whereas domain II stabilizes the L1-rRNA complex.

INTRODUCTION

Ribosomal protein L1 is located on the side protuberance opposite the L7/L12 stalk of the 50S ribosomal subunit. In bacteria and archaea, L1 has a dual function, as a primary RNA-binding protein (1,2) and as a translational repressor of its own synthesis (3–5).

Earlier, we have determined the crystal structures of L1 proteins from the bacterium *Thermus thermophilus* (TthL1), and from the archaea *Methanococcus jannaschii* (MjaL1) and *Methanococcus thermolithotrophicus* (MthL1) (6–8). The models showed that L1 is a two-domain protein, whose N- and C-termini are located close to each other in domain I. The central part of the polypeptide chain protrudes from domain I and folds in domain II. The two domains are connected by a hinge region that consists of two oppositely directed polypeptide chains, which have a different length.

L1 proteins, which show a very high affinity for RNA, e.g. MjaL1 and MthL1 (5,9), have a large interdomain cavity in the isolated and the RNA-bound forms, the two domains are well separated from each other; this conformation is designated as the 'open' conformation. The flexible hinge region of TthL1 permits the domain movement and allows the protein to adopt the 'closed' or 'open' conformation. The structure of isolated TthL1 is characterized by a 'closed' conformation, with the two domains in close contact.

A comparison of the known crystal structures of isolated L1 from the three different species mentioned earlier revealed two structurally invariant regions on the protein surface, which were suggested to represent its RNA-binding sites (6–8). Each domain possesses one of these binding sites. In the 'closed' conformation of TthL1, the regions binding RNA are inaccessible to RNA (6). Significant opening of the cavity between the two domains increases the distance between the two RNA-binding sites up to 25 Å and makes L1 able to bind RNA.

The model of the hybrid complex between L1 from *Sulfolobus acidocaldarius* (SacL1) and a specific 55 nt fragment of 23S rRNA from *T. thermophilus* confirmed that L1 interacts with rRNA through both conserved regions (10). The structure of archaeal L1 from *M. jannaschii* complexed with its target on the auto-regulatory mRNA (11) also showed two sites of interaction. Nevertheless, the number of residues that contact the RNA is substantially lower in domain II than in domain I,

*To whom correspondence should be addressed. Tel: +43 512 9003-70331; Fax: +43 512 9003-73110; Email: wolfgang.piendl@i-med.ac.at

particularly in the L1-mRNA complex. Later, the structures of two hybrid complexes between bacterial L1 from *T. thermophilus* and mRNA fragments of different length from the archaeon *Methanococcus vannielii* were solved. Crystals of L1 in complex with the 38 nt mRNA fragment contained four copies of the complex in the asymmetric unit. Domain I of the protein interacted with RNA in all four copies, whereas contacts between domain II and RNA were observed only in one of them due to a slightly different mutual orientation of the L1 domains (12). In the structure of the other complex of TthL1 with the 36 nt mRNA fragment only domain I contacts RNA (13). Detailed analysis of L1-RNA interfaces has shown that the conserved region on the surface of domain I of the protein interacts with the structural motif, which is invariant in ribosomal and messenger RNAs. Based on the crystal structures of the mRNA-L1 and rRNA-L1 complexes, we suggested that domain I of L1 is necessary and sufficient for mRNA binding, whereas domain II is required for the higher affinity of L1 for its specific rRNA target site. The regulatory protein L1 is a primary rRNA-binding protein, which binds preferentially to its rRNA binding site and, when in excess, can bind to the regulatory binding site on the mRNA, thereby inhibiting translation of the operon. The difference of more than one order of magnitude observed between the apparent dissociation constants of L1 proteins to their own mRNA and 23S rRNA (5,9) is a prerequisite for a feedback inhibition based on direct competition between the two binding sites (14).

In the L1 sequence, domain II is an insert in domain I. In the structure of the protein, two domains are connected by a hinge region that consists of two oppositely directed polypeptide chains. To test our hypothesis that domain II is not required for specific RNA-binding, we constructed a mutant form of TthL1 where domain II was completely deleted. The isolated domain I was crystallized and its structure was determined. Despite the fact that two parts of the polypeptide chain of domain I were connected directly without the insertion of domain II, the spatial structure of domain I in the isolated form was essentially the same as its structure within the intact protein. RNA-binding experiments showed that the isolated domain I forms stable complexes with specific fragments of both rRNA and mRNA. Moreover, the isolated domain I and intact TthL1 revealed a similar affinity for mRNA. From these results, we conclude that domain I is really sufficient for the recognition of L1 specific target sites on rRNA and mRNA.

MATERIALS AND METHODS

Plasmid constructions

For the overexpression of TthL1 in *Escherichia coli*, a new expression plasmid was constructed. A DNA fragment encoding TthL1 flanked by a 5′-NdeI and a 3′-HindIII site was generated by standard PCR with the primers NdeI-TthL1-fwd (5′-GGAGATATCATATGCCCAAGC ACGG-3′) and HindIII-TthL1-rev (5′-AACTGAATAAG CTTTAGGAGTGGGG-3′) using *T. thermophilus* genomic DNA as a template and cloned into the high-level expression vector pET11a (15), resulting in pTthL1.4. To clone the sequence corresponding to domain I in the TthL1 gene, we used an overlap extension PCR-based site-directed mutagenesis method (16). pTthL1.4 was used as a template in the PCR reactions. The primers used were 5′-TTCCCCACGGCGG GCGGATTGAGTTCCGCAACG-3′ (sense, corresponding to positions 195–205 and 475–496 of the TthL1 coding sequence) and 5′-CCGCCCGCCGTGGGGAGACGGT GCC-3′ (antisense, corresponding to positions 182–205 and 475–480 of the TthL1 coding sequence) and the flanking sequence primers XbaI-pET-fwd (GGGGAA TTGCGAGCGGATAACAATTCC-3′) and HindIII-pET-rev (5′-CTCATGTTTGACAGCTTATCATCGAT AAGC-3′). The resulting final PCR product encoding domain I of TthL1 was cloned into vector pET11a. The nucleotide sequences of the cloned genes were verified by DNA sequencing.

Protein overproduction and purification

The isolated domain I of TthL1 was overproduced in *E.coli* strain BL21(DE3) as a host. Purification of the recombinant domain I was performed by the same procedure as purification of the intact TthL1 (6) with minor modifications. After the final chromatography step, fractions containing the pure protein were pooled and dialyzed into 30 mM Tris–HCl ($pH_{25°C}$ 7.5), 60 mM KCl and concentrated to 10–20 mg/ml using Vivaspin concentrators.

Preparation of RNA fragments

The 36 nt mRNA fragment (13) and the 55 nt rRNA fragment, respectively, used in L1-RNA complex formation were synthesized *in vitro* by transcription with T7 RNA polymerase from linearized plasmids as described (10). The RNA fragments were purified by electrophoresis on 12% polyacrylamide gels (19 : 1 acrylamide/*bis*-acrylamide) containing 7 M urea in a buffer containing 90 mM Tris–borate (pH 8.2) and 1 mM Na_2EDTA. The RNA fragments were eluted with 50 mM Tris–HCl ($pH_{25°C}$ 7.5), 1 mM Na_2EDTA, purified by anion-exchange chromatography, precipitated by ethanol and dissolved in buffer A [30 mM Tris–HCl ($pH_{25°C}$ 7.5), 350 mM KCl, 2 mM $MgCl_2$].

RNA–protein complex formation and PAGE under non-denaturing conditions

The intact TthL1 and the domain I were dialyzed into buffer A. The RNA fragments (in buffer A) were heated at 60°C for 10 min and incubated for a further 10 min at 4°C. To form TthL1–RNA and domain I–RNA complexes, respectively, the proteins were added to RNA and the mixture was incubated for 20 min at 22°C. To investigate a competition of the intact TthL1 and its domain I for RNA binding, the isolated domain I was added to preformed complexes of intact TthL1 with mRNA and rRNA, respectively, then the mixtures were incubated for 20 min at room temperature. RNA–protein complexes were analyzed by electrophoresis using the Mini-PROTEAN

II system (Bio-Rad) on 12% gels under non-denaturing conditions in a buffer containing 90 mM Tris–boric acid (pH 8.2) and 2 mM $MgCl_2$ at 100 V for 2.5 h. After electrophoresis, the gels were stained with toluidine blue O (Sigma).

Crystallization

Crystallization experiments were performed at 6°C by the hanging drop vapor diffusion method on siliconized glass cover slides in Linbro plates. Two microliter drops of the protein solution at 20 mg/ml in 30 mM Tris–HCl (pH25°C 7.5), 60 mM KCl were mixed with 2 µl of different precipitants and equilibrated against the same precipitants. Crystals appeared after 2–3 days in #17 and #22 of Hampton Research Crystal Screen precipitant solutions and grew to a maximum size within 1 week. Before freezing in liquid nitrogen, the crystals were transferred to the corresponding precipitant solutions.

Data collection and structure determination

The isolated domain I of TthL1 was crystallized in two-space groups $P2_1$ and $P3_1$. Data for each of two groups were collected from a single crystal using micro-diffractometer MD2 (spot size $25 \times 5\,\mu^2$) at the SLS synchrotron (Switzerland) in-vacuum undulator beamline X06SA, which is equipped with dynamically bendable mirrors, Si(111) double crystal monochromator and marCCD detector. Data were processed and merged with the XDS program suite (17). Both structures were solved by the molecular replacement method using the structure of domain I of the intact TthL1 (6) as a search model.

Crystals belonging to space group $P2_1$ diffracted to 2.55 Å resolution. For structure amplitudes measured from such a crystal clear solution of the phase problem was obtained by PHASER (18). The electron density map was of good quality and enabled us to build a model of the isolated domain I of TthL1 except eight N-terminal residues. The initial model was subjected to several rounds of a computational refinement and map calculation with REFMAC (19) combined with a manual model inspection and modification with COOT (20). The final model, including 129 amino acid residues, was refined to an R-factor of 17.7% and an R-free of 27.0%. Data and refinement statistics are summarized in Table 1. The structural data and the coordinates have been deposited in the Protein Data Bank (accession code 2OUM).

Structure determination of the L1 domain I crystallized in space group $P3_1$ encounters an obstacle. Detailed analysis of experimental data with SFCHECK of the CCP4 program suite (21) and DETECT_TWINNING of CNS (22), revealed merohedral twinning with the twin law h + k, −k, −l and twin fraction 0.41 in the crystals. An attempt to improve data with DETWIN of the CCP4 program suite resulted in worse data statistics and noticeably reduced data completeness. Therefore, we used twinned data for the model building and refinement. A clear solution for three molecules in the asymmetric unit was obtained both by AMoRe (23) and PHASER (18). Crystallographic refinement was executed using procedures specified for twinned crystals in CNS (22), and model building was performed with COOT (20). Non-crystallographic symmetry restraints were used during the early stages of refinement, but all molecules in the asymmetric unit were finally refined separately. The final model refined to an R-factor of 19.3% and R-free of 23.3%, includes three molecules of the isolated domain I and 152 water molecules. The structural data and the coordinates have been deposited in the Protein Data Bank (accession code 2OV7). Data and refinement statistics are summarized in Table 1.

Table 1. Data collection and refinement statistics

Crystallographic data[a,b]		
Space group	$P2_1$	$P3_1$
Unit-cell parameters (Å, °)	a = 31.7, b = 45.3, c = 37.9; α = 90.0, β = 100.7, γ = 90.0	a = 79.2, b = 79.2, c = 47.6; α = 90.0, β = 90.0, γ = 120.0
Wavelength (Å)	0.95	0.95
Resolution (Å)	15.0–2.55 (2.60–2.55)	15.0–2.30 (2.40–2.30)
Number of reflections	11175 (531)	65385 (7800)
Number of unique reflections	3392 (180)	14608 (1754)
Completeness (%)	94.4 (89.1)	96.8 (98.4)
Averaged redundancy	3.3 (3.0)	4.6 (4.4)
$I/\sigma_i(I)$	8.8 (3.5)	7.9 (3.2)
$R_{sym}(I)$ (%)[b]	11.9 (35.1)	13.9 (46.1)
Refinement statistics		
Resolution range (Å)	15.0–2.55 (2.62–2.55)	15–2.30 (2.40–2.30)
Reflections	3356 (241)	14468 (1476)
R-factor (%)	17.7 (22.7)	19.3 (21.0)
Free R-factor (%)	27.0 (38.9)	23.3 (23.4)
Mean B-value (overall, Å^2)	34.3	60.7
r.m.s. deviation		
Bond lengths (Å)	0.010	0.006
Bond angles (°)	1.3	0.8

[a]Data collected at 100K.
[b]Values in parenthesis are statistics for the highest resolution shell.

RESULTS AND DISCUSSION

Crystal structure of the isolated domain I of TthL1

In TthL1, the hinge region contains residues 66–71 and 159–160 (Figure 1A). In the open conformation of TthL1, two glycines (Gly67 and Gly159) located in the oppositely directed chains are about 4 Å apart, a distance that allows a peptide bond formation between the two glycines. Therefore, the positions of these glycines are most suitable as endpoints to delete the central part of the polypeptide chain, which forms domain II. The isolated domain I containing amino acid residues 1–67 and 159–228 (the numbers correspond to the intact TthL1 protein) was overproduced in *E.coli* cells, purified and crystallized.

Here, we report two structures of the isolated domain I of ribosomal protein L1 from *T. thermophilus* crystallized in space groups $P2_1$ and $P3_1$. Both structures have the same fold. An overall view of the model is shown in Figure 1. The isolated domain I has a two-layer structure. One of the layers is formed by a four-stranded anti-parallel β-sheet

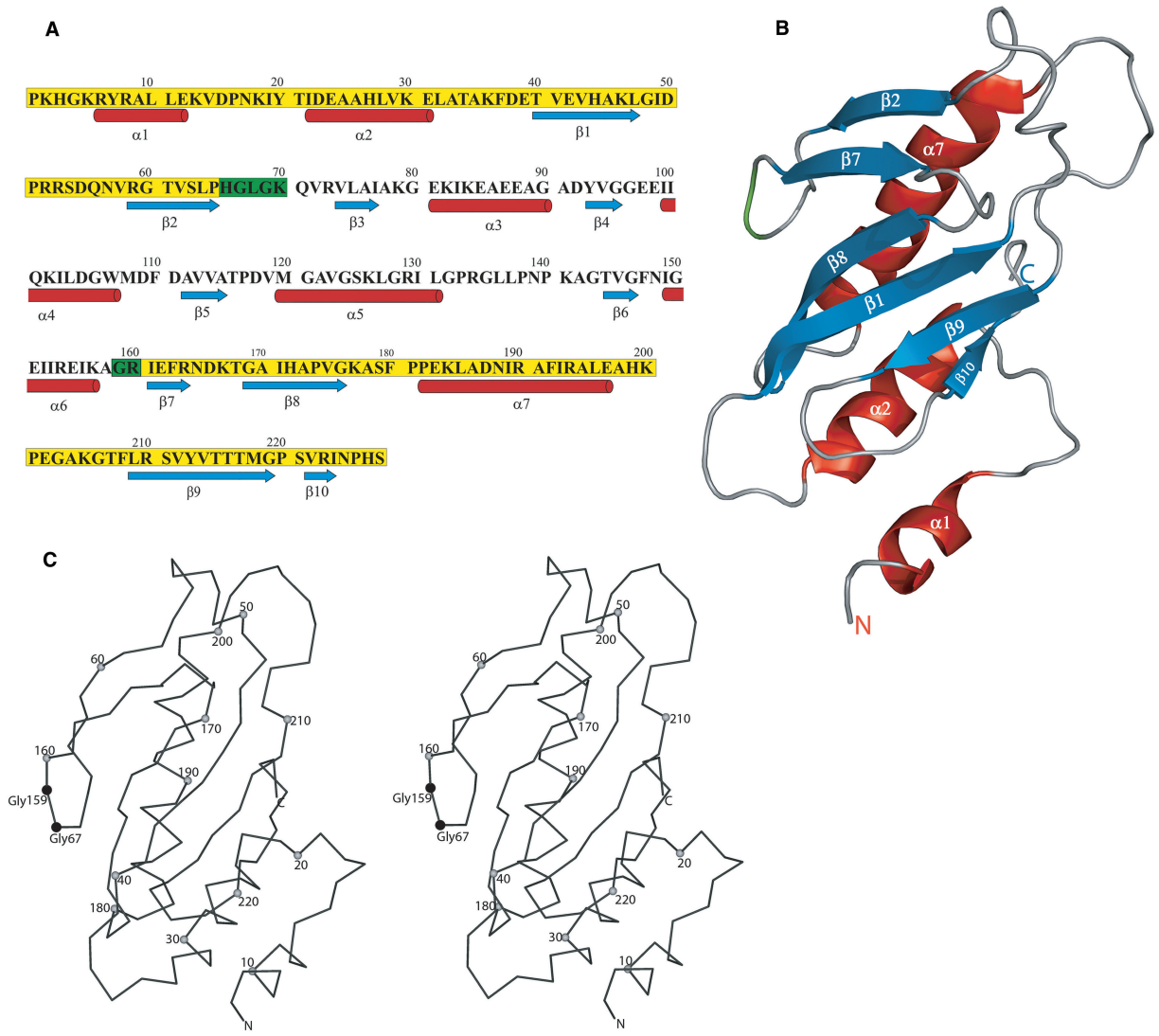

Figure 1. (**A**) Sequence of the *T. thermophilus* L1 protein. Residues of domain I and the hinge region are shown with yellow and green background, respectively. The α-helices are indicated as red cylinders, β-strands as blue arrows. (**B**) Schematic representation of the structure of the isolated domain I of TthL1. The numbering of α-helices (red) and β-strands (blue) corresponds to that of the entire TthL1. (**C**) Stereo view of a Cα trace of the isolated domain I of TthL1.

(β1,β8,β9 and β10), the other contains two α-helices (α2 and α7). The N-terminal α-helix (α1) shields the interlayer region from one side, whereas two anti-parallel β-strands (β2 and β7) cover it from the other side. The loop connecting these strands contains two glycine residues, which form a peptide bond and connect the two parts of the polypeptide chain folded into domain I.

Comparison of the structures of four molecules, one in the asymmetric unit of the crystal belonging to space group $P2_1$ (K) and three in the asymmetric unit of the crystal belonging to space group $P3_1$ (A, B, C), revealed the most flexible parts of the protein. It turned out that eight N-terminal residues are flexible and could not be traced in the electron density maps. Besides, residues of loops 30–39, 50–57 and 200–208 have faint electron density and differ in all obtained structures. Thus, the loop 30–39 has two possible conformations characterized by alternative change of torsion angles of residues Thr34 and Ala35. One of these conformations is realized in molecules K and B, the other in molecules A and C. Disregarding these flexible loops, all models have similar conformations with an r.m.s. deviation between Cα atoms of about 0.5 Å. Superposition of the entire structures increases this value to >1.0 Å. Detailed analysis of the crystal packing revealed that amino acid residues of the flexible loops are involved in crystal contacts, which vary for all four analyzed molecules. Moreover, intermolecular contacts of molecule K induce the displacement of the functionally significant loop 215–225.

Comparison of the structures of the intact TthL1 and its isolated domain I

Earlier, we have published the crystal structure of ribosomal protein L1 from *T. thermophilus* in free form

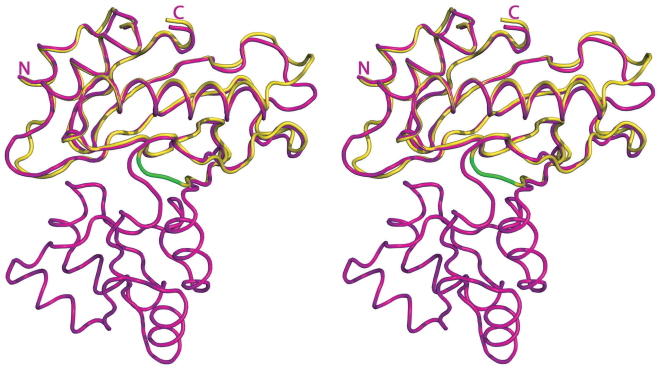

Figure 2. Superposition of the structures of the isolated domain I (yellow) and entire TthL1 protein (magenta) with least squares minimization of differences in Cα atom coordinates of domain I. Connection of two glycines located in anti-parallel chains is shown in green.

(6) and in complex with mRNA (12,13). A comparison of the structure of domain I as part of the intact protein and that of the isolated domain I revealed that the overall 3D structures are closely related (Figure 2). Only the regions of flexible loops involved in crystal contacts show some differences. Structures of domain I within the intact TthL1 and in the isolated state (molecule A) were superimposed with an r.m.s. deviation of 0.934 Å for all Cα atoms. Disregarding two flexible loops, superposition of these structures yielded an r.m.s. deviation of 0.485 Å. Interestingly, the conformation of the interdomain connection and that of the adjacent two β-strands of domain I is quite different in the open and closed form of TthL1. In the isolated domain I, the location of the β-strands is the same as in the open conformation of TthL1. Hydrogen bonds between these strands are identical. The long chain of the interdomain connection decreases in length to two residues 66–67. Residue 66 retains the same position as in the intact molecule, but residues 67 and 159 slightly move toward each other to form a peptide bond. It also results in displacement of residues 160–161. Thus, the isolated domain I has the same crystal structure as domain I within the intact TthL1 despite the fact that 91 amino acid residues of the protein located in the central part of its amino acid sequence were deleted.

Interaction of the isolated domain I with ribosomal and messenger RNAs

Initial filter binding experiments to test the affinity of the isolated TthL1 domain I for its specific rRNA and mRNA target site failed. We assume that TthL1 domain I does not bind to nitrocellulose membranes. Therefore, we had to resort to electrophoretic mobility shift assays. To test the affinity of TthL1 domain I for rRNA, we used a specific 55-nucleotide fragment of 23S rRNA from *T. thermophilus*. Earlier, the crystal structure of the same RNA fragment complexed with intact L1 from *S. acidocaldarius* was determined (10). To test the specific affinity of the isolated domain I for mRNA, we used a 36-nucleotide fragment of mRNA from *M. vannielii* carrying the specific regulatory L1 binding site.

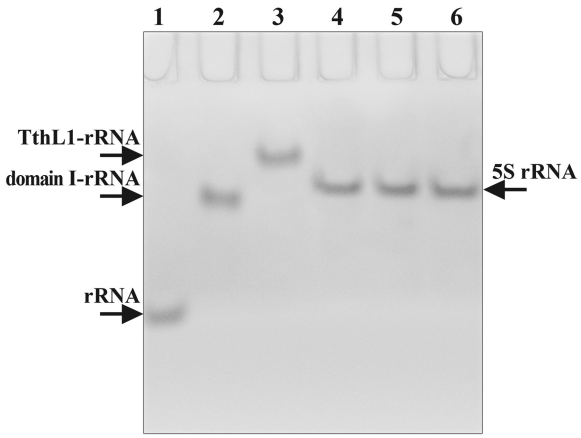

Figure 3. Interaction of the isolated domain I and intact TthL1 with the specific rRNA fragment, analyzed by non-denaturing PAGE. 1, 55 nt rRNA fragment; 2, rRNA, mixed with domain I in a molar ratio of 1:1; 3, rRNA mixed with intact TthL1 in a molar ratio of 1:1; 4, 5S rRNA; 5, 5S rRNA mixed with domain I in a molar ratio of 1:1; 6, 5S rRNA mixed with intact TthL1 in a molar ratio of 1:1. The RNA and protein concentration in the incubation mixture was 55 μM (lines 2 and 3) and 25 μM (lines 5 and 6), respectively.

In previous experiments, this fragment was used for crystallization and structure determination of the TthL1–mRNA complex (13). The 5S rRNA served as a control to identify non-specific RNA–protein interactions. To minimize potential non-specific interactions, the complex formation was performed in a buffer containing 350 mM KCl. Both TthL1 domain I and the entire TthL1 bind the 23S rRNA completely when mixed in a molar ratio of 1 : 1 (Figure 3, lanes 2 and 3). Neither ThL1 domain I nor TthL1 showed significant binding to the non-cognate 5S rRNA (Figure 3, lanes 5 and 6). Similarly, both proteins bind the specific mRNA fragment (Figure 4, lanes 2 and 5).

Based on the crystal structures of the L1–rRNA and L1–mRNA complexes, we have earlier suggested that domain I would be sufficient for mRNA binding, whereas domain II of L1 is required for the high affinity binding to rRNA. If this assumption is correct, the intact L1 and its isolated domain I should bind mRNA with a more or less identical affinity, whereas affinity of the isolated domain I to the specific rRNA target site should be lower compared to that of the intact protein. To prove this assumption right or wrong, we tested the competition between the isolated domain I and intact TthL1 for binding RNAs (Figure 4). The addition of the isolated domain I to the preformed TthL1–mRNA complex resulted in replacement of the intact protein by the isolated domain I in about half of complexes (Figure 4, lanes 3 and 4). Under the same experimental conditions the isolated domain I replaced the intact protein from the TthL1–rRNA complex to only a small extent (Figure 4, lanes 8 and 9). These results indicate the intact TthL1 and its isolated domain I have a similar or identical affinity for mRNA, while that for rRNA is quite different. TthL1 binds the specific 23S rRNA target site with a much higher affinity compared to its isolated domain I.

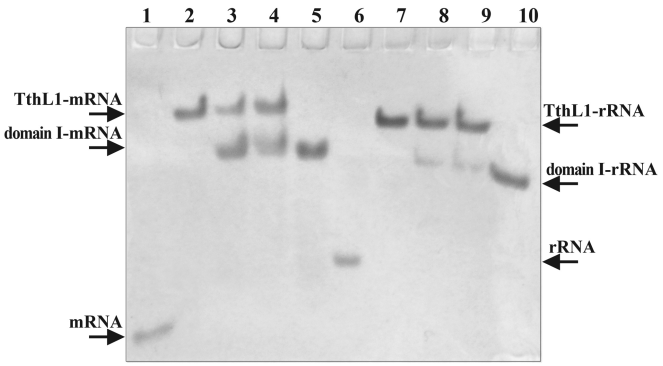

Figure 4. Competition of intact TthL1 and the isolated domain I for binding the specific rRNA and mRNA fragments, analyzed by non-denaturing PAGE. The isolated domain I was added to preformed complexes of the intact TthL1 with mRNA and rRNA. 1, 36 nt mRNA fragment; 2, mRNA-TthL1 complex (molar ratio of 1:1); 3 and 4, mRNA-TthL1 complex mixed with domain I in a molar ratio of 1:1.5 and 1:3, respectively; 5, mRNA-domain I complex (molar ratio of 1:1); 6, 55 nt rRNA fragment; 7, rRNA-TthL1 complex (molar ratio of 1:1); 8 and 9, rRNA-TthL1 complex mixed with domain I in a molar ratio of 1:1.5 and 1:3, respectively; 10, rRNA-domain I complex (molar ratio of 1:1). RNA concentrations in the incubation mixture were: 80 μM for the mRNA fragment and 55 μM for the rRNA fragment. Concentrations of intact TthL1 in the incubation mixture were 80 μM (lines 2–4) and 55 μM (lines 7–9). Concentrations of domain I in the incubation mixture were 240 μM (line 3), 120 μM (line 4), 80 μM (line 5), 82.5 μM (line 8), 165 μM (line 9) and 55 μM (line 10).

We could demonstrate that domain I of ribosomal protein L1 retains its structure in the isolated form and binds specific fragments of ribosomal and messenger RNAs. Moreover, the isolated domain I demonstrates an affinity for mRNA similar to that of the intact protein. This confirms our suggestion that domain I of ribosomal protein L1 plays the essential role in recognizing the specific RNA target sites.

The second domain of L1 provides the additional contact site, which forms hydrogen bonds with ribosomal RNA making the corresponding complex more stable than the L1–mRNA complex. The difference in stability of the ribosomal and regulatory L1–RNA complexes is the basis for negative feed-back regulation of translation by L1.

ACKNOWLEDGEMENTS

The authors thank B. Maguire for critical reading of the article. This work was supported by the Russian Academy of Sciences, the Russian Foundation for Basic Research (No. 05-04-48338); the Program of RAS on Molecular and Cellular Biology and the Program of the RF President on support of outstanding scientific schools; International Research Scholar's award from the Howard Hughes Medical Institute (to M.G.); the Austrian Science Fund (FWF, P17164-B10 to W.P.). Funding to pay the Open Access publication charges for this article was provided by the Austrian Science Fund.

Conflict of interest statement. None declared.

REFERENCES

1. Zimmermann,R.A. (1980) Interactions among protein and RNA components of the ribosome. In Chambliss,G., Craven,G., Davies,J., Davies,K., Kahan,L. and Nomura,M. (eds), *Ribosomes. Structure, Function and Genetics*, University Park Press, Baltimore, pp. 135–169.
2. Gourse,R.L., Thurlow,D.L., Gerbi,S.A. and Zimmermann,R.A. (1981) Specific binding of a prokaryotic ribosomal protein to a eukaryotic ribosomal RNA: implications for evolution and autoregulation. *Proc. Natl Acad. Sci. USA*, **78**, 2722–2726.
3. Gourse,R., Sharrock,R. and Nomura,M. (1986) Control of ribosome synthesis in *Escherihia coli*. In Hardesty,B. and Kramer,G. (eds), *Structure, Function, and Genetics in Ribosomes*, Springer, NewYork, pp. 766–788.
4. Mayer,C., Köhrer,C., Gröbner,P. and Piendl,W. (1998) MvaL1 autoregulates the synthesis of the three ribosomal proteins encoded on the MvaL1 operon of the archaeon *Methanococcus vannielii* by inhibiting its own translation before or at the formation of the fist peptide bond. *Mol. Microbiol.*, **27**, 455–468.
5. Kraft,A., Lutz,C., Lingenhel,A., Gröbner,P. and Piendl,W. (1999) Control of ribosomal protein L1 synthesis in mesophilic and thermophilic archaea. *Genetics*, **152**, 1363–1372.
6. Nikonov,S., Nevskaya,N., Eliseikina,I., Fomenkova,N., Nikulin,A., Ossina,N., Garber,M., Jonsson,B.-H., Briand,C. *et al.* (1996) Crystal structure of the RNA-binding ribosomal protein L1 from *Thermus thermophilus*. *EMBO J.*, **15**, 1350–1359.
7. Nevskaya,N., Tishchenko,S., Fedorov,R., Al-Karadaghi,S., Lilyas,A., Kraft,A., Piendl,W., Garber,M. and Nikonov,S. (2000) Archaeal ribosomal protein L1: the structure provides new insights into RNA binding of the L1 protein family. *Structure*, **8**, 363–371.
8. Nevskaya,N., Tishchenko,S., Paveliev,M., Smolinskaya,Yu., Fedorov,R., Piendl,W., Nakamura,Y., Toyoda,T., Garber,M. *et al.* (2002) Structure of ribosomal protein L1 from *Methanococcus thermolithotrophicus*. Functionally important structural invariants on the L1 surface. *Acta Crystallogr.*, **D58**, 1023–1029.
9. Köhrer,C., Mayer,C., Neumair,O., Gröbner,P. and Piendl,W. (1998) Interaction of ribosomal L1 proteins from mesophilic and thermophilic archaea and bacteria with specific L1-binding sites on 23SrRNA and mRNA. *Eur. J. Biochem.*, **256**, 97–105.
10. Nikulin,A., Eliseikina,I., Tishchenko,S., Nevskaya,N., Davydova,N., Platonova,O., Piendl,W., Selmer,M., Liljas,A. *et al.* (2003) Structure of the L1 protuberance in the ribosome. *Nature Struct. Biol.*, **10**, 104–108.
11. Nevskaya,N., Tishchenko,S., Gabdoulkhakov,A., Nikonova,E., Nikonov,O., Nikulin,A., Platonova,O., Garber,M., Nikonov,S. *et al.* (2005) Ribosomal protein L1 recognizes the same specific structural motif in its target sites on the autoregulatory mRNA and 23S rRNA. *Nucleic Acids Res.*, **33**, 478–485.
12. Nevskaya,N., Tishchenko,S., Volchkov,S., Kljashtorny,V., Nikonova,E., Nikonov,O., Nikulin,A., Köhrer,C., Piendl,W. *et al.* (2006) New insights into the interaction of ribosomal protein L1 with RNA. *J. Mol. Biol.*, **355**, 747–759.
13. Tishchenko,S., Nikonova,E., Nikulin,A., Nevskaya,N., Volchkov,S., Piendl,W., Garber,M. and Nikonov,S. (2006) Structure of the ribosomal protein L1-mRNA complex at 2.1 Å resolution: common features of crystal packing of L1-RNA complexes. *Acta Crystallogr.*, **D62**, 1545–1554.
14. Zengel,J.M. and Lindahl,L. (1994) Diverse mechanisms for regulating ribosomal protein synthesis in *Escherichia coli*. *Prog. Nucleic Acid Res. Mol. Biol.*, **47**, 331–370.
15. Dubendorff,J.W. and Studier,F.W. (1991) Creation of a T7 autogene. Cloning and expression of the gene for bacteriophage T7 RNA polymerase under control of its cognate promoter. *J. Mol. Biol.*, **219**, 61–68.
16. Ho,S.N., Hunt., H.D. Horton,R.M., Pullen,J.K. and Pease,L.R. (1989) Site-directed mutagenesis by overlap extension using the polymerase chain reaction. *Gene*, **77**, 51–59.
17. Kabsch,W. (2001) Integration, scaling, space-group assignment and post refinement. In Rossmann,M.G. and Arnold,E. (eds), *International Tables for Crystallography*, Springer for the International Union of Crystallography, New York, pp. 218–225.

18. Storoni,L.C., McCoy,A.J. and Read,R.J. (2004) Likelihood-enhanced fast rotation functions. *Acta Crystallogr.*, **D60**, 432–438.
19. Murshudov,G.N., Vagin,A.A. and Dodson,E.J. (1997) Refinement of macromolecular structures by the maximum-likelihood method. *Acta Crystallogr.*, **D57**, 240–255.
20. Emsley,P. and Cowtan,K. (2004) Coot: model-building tools for molecular graphics. *Acta Crystallogr.*, **D60**, 2126–2132.
21. Bailey,S. (1994) The CCP4 suite: programs for protein crystallography. *Acta Crystallogr.*, **D50**, 760–763.
22. Brünger,A.T., Adams,P.D., Clore,G.M., DeLano,W.L., Gros,P., Grosse-Kunstleve,R.W., Jiang,J.-S., Kuszewski,J., Nilges,M. *et al.* (1998) Crystallography and NMR system: a new software suite for macromolecular structure determination. *Acta Crystallogr.*, **D54**, 905–921.
23. Navaza,J. (1994) AmoRe: an automated package for molecular replacement. *Acta Crystallogr.*, **A50**, 157–163.